Glucose production during an IVGTT by deconvolution: validation with the tracer-to-tracee clamp technique

Paolo Vicini, Jeffrey J. Zachwieja, Kevin E. Yarasheski, Dennis M. Bier, Andrea Caumo and Claudio Cobelli

Am J Physiol Endocrinol Metab 276:E285-E294, 1999.

AJP - Endocrinology and Metabolism publishes results of original studies about endocrine and metabolic systems on any level of organization. It is published 12 times a year (monthly) by the American Physiological Society, 9650 Rockville Pike, Bethesda MD 20814-3991. ISSN: 0193-1849, ESSN: 1522-1555. Visit our website at http://www.the-aps.org/.

Glucose production during an IVGTT by deconvolution: validation with the tracer-to-tracee clamp technique

PAOLO VICINI,[1] JEFFREY J. ZACHWIEJA,[2,3] KEVIN E. YARASHESKI,[2]
DENNIS M. BIER,[4] ANDREA CAUMO,[5] AND CLAUDIO COBELLI[1]
[1]*Department of Electronics and Informatics, University of Padova, 35131 Padova;* [5]*Scientific Institute San Raffaele, 20132 Milano, Italy;* [2]*Metabolism Division, Washington University School of Medicine, Saint Louis, Missouri 63110;* [3]*Pennington Biomedical Research Center, Baton Rouge, Louisiana 70808; and* [4]*Children's Nutrition Research Center, Baylor College of Medicine, Houston, Texas 77030-2600*

Vicini, Paolo, Jeffrey J. Zachwieja, Kevin E. Yarasheski, Dennis M. Bier, Andrea Caumo, and Claudio Cobelli. Glucose production during an IVGTT by deconvolution: validation with the tracer-to-tracee clamp technique. *Am. J. Physiol.* 276 (*Endocrinol. Metab.* 39): E285–E294, 1999.—Recently, a new method, based on a two-compartment minimal model and deconvolution [A. Caumo and C. Cobelli. *Am. J. Physiol* 264 (*Endocrinol. Metab.*. 37): E829–E841, 1993; P. Vicini, G. Sparacino, A. Caumo, and C. Cobelli. *Comput. Meth. Prog. Biomed.* 52: 147–156, 1997], has been proposed to estimate endogenous glucose production (EGP) from labeled intravenous glucose tolerance test (IVGTT) data. Our aim here is to compare this EGP profile with that independently obtained with the reference method, based on the tracer-to-tracee ratio (TTR) clamp. An insulin-modified (0.03 U/kg body wt infused over 5 min) [6,6-$^2H_2$]glucose-labeled IVGTT (0.33 g/kg of glucose) was performed in 10 normal subjects. A second tracer ([U-^{13}C]glucose) was also infused during the test in a variable fashion to clamp endogenous glucose TTR. The TTR clamp was quite successful. As a result, the EGP profile, reconstructed from [U-^{13}C]glucose data with the models of Steele and Radziuk, were almost superimposable. The deconvolution-obtained EGP profile, calculated from [6,6-$^2H_2$]glucose data, showed remarkable agreement with that obtained from the TTR clamp. Some differences between the two profiles were noted in the estimated basal EGP and in the initial modalities of EGP inhibition. A high interindividual variability was also observed with both methods in the resumption of EGP to baseline; variability was high in both the timing and the extent of resumption. In conclusion, the use of the two-compartment minimal model of the IVGTT and deconvolution allows the estimation of a profile of EGP that is in very good agreement with that independently obtained with a TTR clamp.

nonsteady state; mathematical model; tracer-to-tracee ratio; specific activity clamp

THE LABELED INTRAVENOUS GLUCOSE TOLERANCE TEST (IVGTT) is a powerful tool to estimate parameters describing glucose metabolism in vivo, in normal and disease states. In particular, it has recently been shown that, if a two-compartment minimal model (2CMM) of labeled glucose kinetics is used to describe the impulse response of the glucose system, it is possible to obtain, via deconvolution, a physiologically plausible profile of endogenous glucose production (EGP) in normal humans during the IVGTT nonsteady state (4, 24), thus eliminating the anomalies previously encountered when a single-compartment minimal model was used (5). This approach was also recently used with success in normal subjects by Overkamp et al. (19). The ability of reliably measuring EGP in nonsteady state is crucial to investigate the modalities of glucose metabolism in normal and disease states, and in particular to elucidate to what extent abnormal regulation of EGP contributes to the fasting hyperglycemia and carbohydrate intolerance associated with non-insulin-dependent diabetes mellitus, obesity, and advancing age.

Validation of this deconvoluted profile of EGP by means of direct measurement, i.e., the arteriovenous (a-v) balance technique, is extremely difficult because the a-v technique is easily applicable only in steady state (26), where the Fick principle (13) is known to hold. In all generality, assessment of EGP in nonsteady state from tracer data must rely on a model of glucose kinetics. However, modeling glucose kinetics in nonsteady state is difficult. General-purpose simplistic models are in use (20, 22); however, as shown by non-steady-state theory (6, 17), they introduce errors. However, theory (6, 17, 18) also shows that, if the glucose specific activity [or the tracer-to-tracee ratio (TTR) for a stable isotope tracer (9)] is kept constant (or, more realistically, its variations are minimized), one can obtain a reliable estimate of EGP regardless of the model used to describe non-steady-state glucose kinetics (6, 18). Clamping glucose specific activity or TTR during an IVGTT is very difficult, because the time course of EGP, besides being unknown, is likely to present noticeable and at least partly unpredictable variations. A pioneering attempt along this line was proposed in the dog by Cowan and Hetenyi (11), a study in which the glucose system was prelabeled with a primed, continuous infusion of tracer that was initiated 100 min before the labeled IVGTT and maintained thereafter; in this way, specific activity reached a constant value before the labeled IVGTT, and its changes during the test were thus reduced.

In the present work, we use the TTR clamp technique to validate the deconvolution method for reconstructing EGP during an IVGTT. To do so, two tracers, [6,6-$^2H_2$]glucose and [U-^{13}C]glucose, were simultaneously injected in the same subject and used to provide, respectively, the deconvolution and the TTR clamp EGP profile.

EXPERIMENTAL DESIGN AND METHODS

Subjects and Protocol

Subjects. Five young men and five young women [age: 27 ± (SE) 7 yr, body weight: 62 ± 3 kg] were studied after an overnight fast. All were healthy, nonmedicated, nondiabetic, in the normal range for height and weight, and free of cardiovascular disease. Before participation, the subjects received instructions from a research dietitian on how to follow a weight-maintaining diet that provided ≥250 g of carbohydrate on each of the 3 days leading up to an experiment. During the day before an experiment, no exercise or organized sport was allowed. All subjects received a detailed description (both verbal and written) of the experimental protocol, they were informed of potential risks, and written informed consent was obtained. This study was approved by the Washington University School of Medicine Institutional Review Board.

Protocol

On the morning of an experiment the subjects were weighed and, starting at 0800, a Teflon catheter was inserted into a forearm vein of both arms, one for blood sampling and the second for infusion of glucose and glucose isotopes. Patency of the catheter used for blood sampling was maintained with a slow drip of sterile saline. The study lasted a total of 6 h for each subject (Fig. 1). After a baseline blood sample was drawn, the subjects received a 2-h (0–120 min) primed (7 mg/kg), constant intravenous infusion (70 $\mu g \cdot kg^{-} \cdot min^{-1}$) of [U-^{13}C]glucose to assess basal EGP. The pump used was a Harvard variable-rate microprocessor-controlled motor-driven syringe infusion pump (Pump 22, South Natick, MA). We calibrated by pumping water at a set rate for a measured time period and measured the weight and volume of the water pumped. This agreed with the rate set on the pump. Also, during the tracer infusion experiment, we marked the syringe volume and clock time each time we changed the infusion rate. We could then calculate the volume delivered over a measured period of time (rate) during the actual experiment.

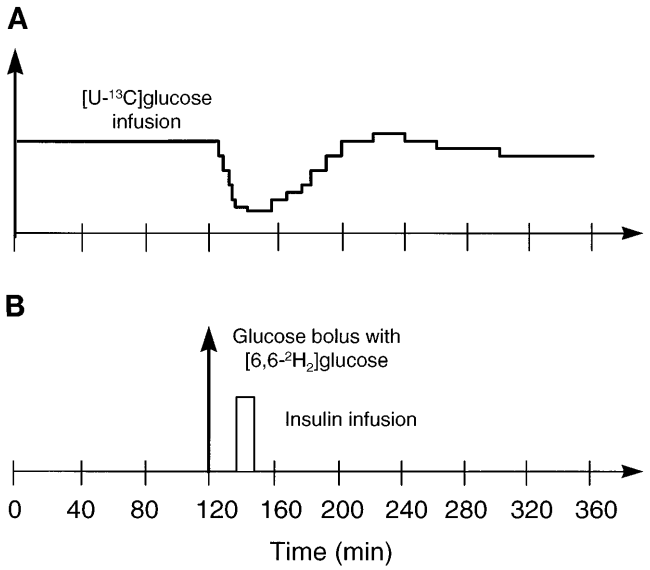

Fig. 1. Experimental protocol. Each subject received simultaneously a variable [U-^{13}C]glucose infusion (*A*) and a [6,6-$^{2}H_2$]glucose-labeled intravenous glucose tolerance test (IVGTT, *B*).

The second part of the experiment consisted of a 4-h (120–360 min) IVGTT (330 mg/kg body wt of exogenous glucose were administered as a bolus at 120 min) labeled with the stable isotope [6,6-$^{2}H_2$]glucose (the concentration of pure [6,6-$^{2}H_2$]glucose in the bolus was 10% of the unlabeled, natural glucose content) and modified with insulin infusion. In humans, the plasma glucose and insulin patterns after glucose injection are quite similar. Therefore, it is difficult to differentiate between the effects of glucose and insulin during an IVGTT, and this ultimately results in increased variability in the minimal model parameter estimates of insulin sensitivity and glucose effectiveness (25). Thus, we modified the stable labeled IVGTT protocol to include a short-term insulin infusion, so that the temporal patterns of glucose and insulin became less similar. To do this, 0.03 U/kg of regular human insulin (Novolin, Novo Nordisk, Princeton, NJ) was infused for 5 min starting at *minute 20* of the IVGTT. During the IVGTT, [U-^{13}C]glucose infusion continued, but the infusion rate was this time adjusted in a stepwise fashion to mimic the predicted pattern of EGP, thus keeping the TTR of [U-^{13}C]glucose (and thus of endogenous glucose) constant. A few pilot experiments were allowed to adjust the stepwise infusion (initially based on the results of Ref. 4), and the following schedule was used (in percentages of basal rate): basal period, 100% of basal infusion rate; 0–2 min, 100%; 2–4 min, 80%; 4–6 min, 60%; 6–8 min, 40%; 8–10 min, 20%; 10–15 min, 10%; 15–30 min, 5%; 30–40 min, 20%; 40–50 min, 30%; 50–55 min, 40%; 55–60 min, 60%; 60–70 min, 80%; 70–80 min, 100%; 80–100 min, 110%; 100–120 min, 100%; 120–160 min, 90%; 160–240 min, 80%. In the event that a blood sample and change in infusion rate occurred at the same time point, blood sampling preceded the change in infusion rate.

Blood samples were obtained at 0, 2, 3, 5, 8, 10, 15, 20, 30, 45, 60, 75, 90, 100, 110, and 120 min during the first part of the experiment and at 122, 123, 124, 125, 126, 128, 130, 132, 134, 136, 139, 142, 144, 146, 148, 150, 155, 160, 165, 170, 175, 180, 190, 200, 220, 240, 260, 280, 300, 330, and 360 min during the IVGTT. Total glucose, plasma insulin, and the complete mass spectra for [U-^{13}C]glucose and [6,6-$^{2}H_2$]glucose were measured from each sample.

Methods

Measurements. Blood samples for glucose and insulin were collected in heparinized tubes. All samples were immediately placed on ice, and after centrifugation, plasma was stored at −80°C for insulin and glucose tracer analysis. Plasma glucose concentration was determined at bedside by the glucose oxidase method using a Beckman Glucose Analyzer (Beckman Instruments, Fullerton, CA), and plasma insulin was determined by radioimmunoassay (16). A portion of each plasma sample was deproteinized in cold acetone. After centrifugation, the supernatant was removed and evaporated, and the pentaacetate derivative of glucose was formed by the addition of 100 µl of acetic anhydride-pyridine (1:1). Glucose was separated by gas chromatography at 180°C on a 3% OV 101 column, and ^{2}H and ^{13}C isotopic abundance was measured by positive chemical ionization mass spectrometry by use of selected ion monitoring of peak intensities at mass-to-charge ratios 331, 332, 333, 334, 335, 336, and 337. The [U-^{13}C]glucose tracer (99 atom%) was manufactured by Isotec (Miamisburg, OH), and the [6,6-$^{2}H_2$]glucose tracer (99 atom%) was manufactured by MassTrace (Woburn, MA). The gas chromatography-mass spectrometer (GC-MS) characteristics and manufacturer were Finnigan 3300 GC-quadrupole-MS (Sunnyvale, NY).

The TTR of [6,6-$^2H_2$]glucose [$Z_I(t)$] and [U-^{13}C]glucose [$Z_{II}(t)$] at each sampling time t were calculated from the peak ratio data by using an extension of the case of multiple labels of the formulas in Refs. 8–10. From the TTRs, $Z_I(t)$ and $Z_{II}(t)$ and total glucose $G(t)$, one can derive the concentrations of exogenous glucose injected with the [6,6-$^2H_2$]glucose-enriched bolus in the sample

$$C_I(t) = \frac{G(t)Z_I(t)}{1 + Z_I(t) + Z_{II}(t)} \quad (1)$$

and of exogenous glucose injected with the [U-^{13}C]glucose-enriched bolus

$$C_{II}(t) = \frac{G(t)Z_{II}(t)}{1 + Z_I(t) + Z_{II}(t)} \quad (2)$$

In the following explanation, we will refer to [6,6-$^2H_2$]glucose and [U-^{13}C]glucose concentrations, meaning by this the "total exogenous concentration" injected with these tracers, in keeping with an established formalism (1, 9, 10, 23, 24).

Endogenous glucose, i.e., the portion of plasma glucose concentration attributable to EGP, was calculated from $Z_I(t)$, $Z_{II}(t)$, and total glucose concentration $G(t)$ (7, 9)

$$G_e(t) = G(t) - C_I(t) - C_{II}(t) = \frac{G(t)}{1 + Z_I(t) + Z_{II}(t)} \quad (3)$$

The measurement error associated with all these variables was directly derived via error propagation by use of an extension of the formulas described in Refs. 1 and 10.

EGP estimation from the TTR clamp. From non-steady-state theory (6, 17, 18) we can see that, if the TTR in the accessible compartment is kept constant, $Z_{II}(t) = Z_{II}$, all peripheral compartments that exchange material with the accessible compartment will have the same TTR as the accessible compartment and EGP can be calculated in a model-independent way as follows

$$EGP(t) = \frac{R_a^*(t)}{Z_{II}} \quad (4)$$

$EGP(t)$ is thus equal to the known time-varying tracer infusion rate $R_a^*(t)$, apart from the scale factor given by the constant TTR. It is, however, quite difficult, in practice, to maintain the TTR perfectly constant throughout the experiment, and $EGP(t)$ estimation still requires a model. Nevertheless, by keeping the variations of $Z_{II}(t)$ small, one greatly enhances the accuracy of the model reconstruction of EGP and makes it much less dependent on the validity of the model used. Because in our experiment the TTR clamp was quite good (in Fig. 2 it can be seen how [U-^{13}C]glucose concentration profile in plasma closely followed that of endogenous glucose), we were confident that the non-steady-state error was minimized and that determination of EGP was almost model independent. As a matter of fact, the estimates of EGP provided by models of Steele (22) and Radziuk et al. (20), i.e., the two models that are widely used to perform non-steady-state analysis, were almost identical (as we will show later on). We chose the EGP profile calculated with Radziuk's two-compartment model because it is more accurate than Steele's model (6, 20). Specifically, we adopted the version of Radziuk's model with only one time-varying irreversible loss from the accessible compartment (20), because it allows us to express the unknown EGP with a simple formula (see APPENDIX A for details)

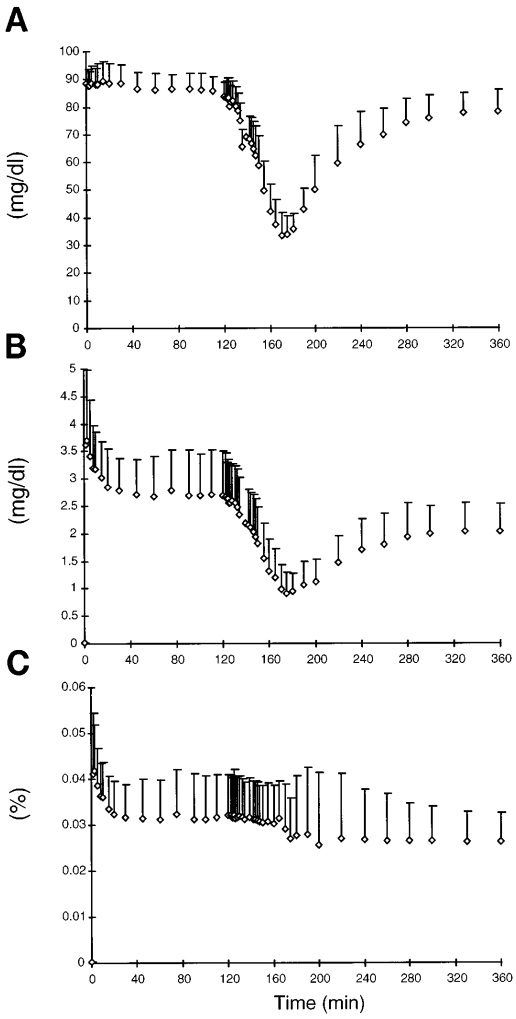

Fig. 2. Mean tracer-to-tracee ratio (TTR) clamp plasma data. *A*: endogenous glucose concentration; *B*: [U-^{13}C]glucose concentration; *C*: endogenous glucose TTR (Z_{II}).

$$EGP(t) = \frac{R_a^*(t)}{Z_{II}(t)} - \frac{V_1 G_e(t)}{Z_{II}(t)} \frac{dZ_{II}(t)}{dt} + k_{12}\left[\frac{q_2^*(t)}{Z_{II}(t)} - q_2(t)\right] \quad (5)$$

where V_1 is the volume of the accessible pool (dl/kg), and q_2 denotes the endogenous glucose mass in the second compartment (mg/kg). Still, although all of the elements in *Eq. 5* can be directly evaluated from data, which makes it particularly appealing, experimental noise can jeopardize some calculations, especially the first derivative of $Z_{II}(t)$, which is evaluated at the midpoint of each sampling integral via finite differences. For this reason, both endogenous glucose and TTR data were smoothed by using a three-samples moving average. In this fashion, we set forth to calculate for each subject a time course of EGP that is likely to be reliable and can then be used as a reference for validation purposes. Note that $EGP(t)$ is also evaluated at the midpoint of each sampling interval.

EGP estimation by deconvolution. We refer to APPENDIX A for details on the 2CMM and the deconvolution approach to estimate EGP. Briefly, the relation between EGP (input) and

endogenous glucose concentration G_e (output) during an IVGTT can be described by the integral equation

$$G_e(t) = \int_0^t h(t,\tau)\,EGP(\tau)\,d\tau + G_b \qquad (6)$$

where G_b is baseline glucose concentration, and $h(t,\tau)$ is the time-varying kernel of the glucose system described by the 2CMM identified from [6,6-$^2H_2$]glucose data. Details of the procedure used for estimation of EGP are reported in Refs. 12 and 24. We wish to point out that *Eq. 6* is a Fredholm integral equation of the first kind, but we use here the term "deconvolution" [rigorously applicable only when the kernel $h(t,\tau)$ is time invariant] both for the sake of simplicity and in keeping with the existing literature (4, 24). EGP is estimated by the following formula

$$EGP = (\mathbf{H}^T\mathbf{B}^{-1}\mathbf{H} + \gamma\mathbf{F}^T\mathbf{F})^{-1}\,\mathbf{H}^T\mathbf{B}^{-1}\Delta G_e + EGP_b \qquad (7)$$

where **H** is the system matrix, **F** is an appropriately chosen regularization matrix (chosen according to the desired degree of smoothness of the EGP estimate; see Refs. 12, 21, and 24 for details), ΔG_e is the deviation of endogenous glucose from baseline, **B** is the (diagonal) matrix of measurement errors associated with endogenous glucose samples, EGP_b is basal EGP, and γ is a regularization parameter.

RESULTS AND DISCUSSION

Basal pretest plasma glucose was 88 ± 6 (SE) mg/dl, and basal pretest plasma insulin concentration was 4 ± 1 μU/ml. Mean plasma [U-^{13}C]glucose concentration (C_{II}) and endogenous glucose TTR (Z_{II}) are shown in Fig. 2, together with endogenous glucose concentration (G_e). Mean plasma glucose (G), insulin (I), and [6,6-$^2H_2$]glucose concentrations (C_I) are shown in Fig. 3.

TTR Clamp

Model parameters (V_1, k_{21}, k_{12}, k_{01}) were estimated for each subject (Table 1) by weighted nonlinear least squares from the data of the primed, constant infusion of [U-^{13}C]glucose during the baseline period of 0–120 min. Weights were chosen optimally, i.e., equal to the inverse of the measurement error variance (3). The measurement error associated with the tracer measurements was assumed to be independent, white, Gaussian, with mean zero and a variance generated by error propagation from the peak ratio measurement error variance (10) and ranged between 6 and 10% (higher for lower concentration values). Peak ratio standard deviations were determined via replicate measurements. *Equation 5* was then applied to the data, and the average profile of EGP is shown in Fig. 4.

A rapid and almost complete suppression of EGP was seen only 10–15 min after the glucose challenge and between 20 and 40 min EGP increased rapidly. In this period (120–160 min of the experimental protocol), the TTR clamp was quite good, and we believe that this constitutes evidence that our estimate of EGP is substantially correct, because it means that the shape of EGP during that time closely agreed with that of the variable [U-^{13}C]glucose infusion. Clamping TTR between 200 and 360 min was, however, much more

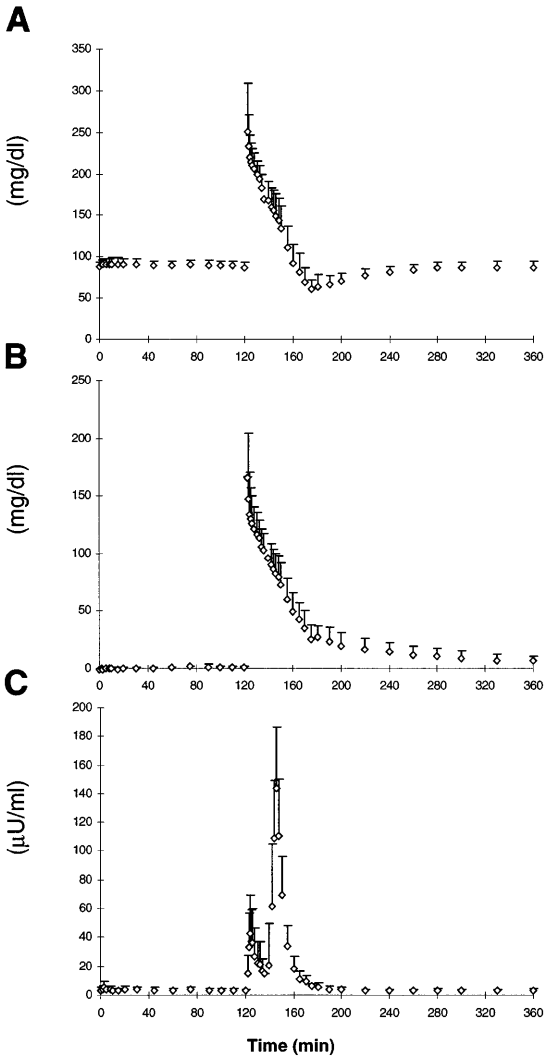

Fig. 3. Mean labeled IVGTT plasma concentration data. *A*: glucose; *B*: [6,6-$^2H_2$]glucose; *C*: insulin.

Table 1. *Parameter values of model of Radziuk et al. (20) identified from data of primed, constant infusion of [U-^{13}C]glucose during baseline period*

Subject No.	V_1, dl/kg	k_{21}, min^{-1}	k_{12}, min^{-1}	k_{01}, min^{-1}
1	1.150 (10)	0.0830 (76)	0.0980 (126)	0.0322 (32)
2	1.538 (3)	0.0312 (15)	0.0495 (18)	0.0169 (5)
3	1.664 (2)	0.0504 (12)	0.0711 (13)	0.0178 (4)
4	1.093 (20)	0.1430 (56)	0.1156 (37)	0.0219 (26)
5	1.837 (10)	0.0209 (95)	0.0559 (116)	0.0179 (19)
6	1.567 (21)	0.0317 (95)	0.0467 (102)	0.0116 (47)
7	1.534 (9)	0.0223 (59)	0.0373 (96)	0.0228 (20)
8	1.246 (12)	0.0495 (50)	0.0591 (54)	0.0253 (17)
9	2.073 (7)	0.0052 (241)	0.0107 (645)	0.0125 (142)
10	1.830 (6)	0.0240 (62)	0.0823 (55)	0.0163 (9)
Mean ±SE	1.553±0.100	0.0461±0.0127	0.0626±0.0096	0.0195±0.0020

Values are parameter estimates. Numbers in parentheses are estimate precisions expressed as percent coefficient of variation (%CV). V_1, volume of glucose accessible pool; k_{21}, k_{12}, k_{01}, glucose kinetic parameters.

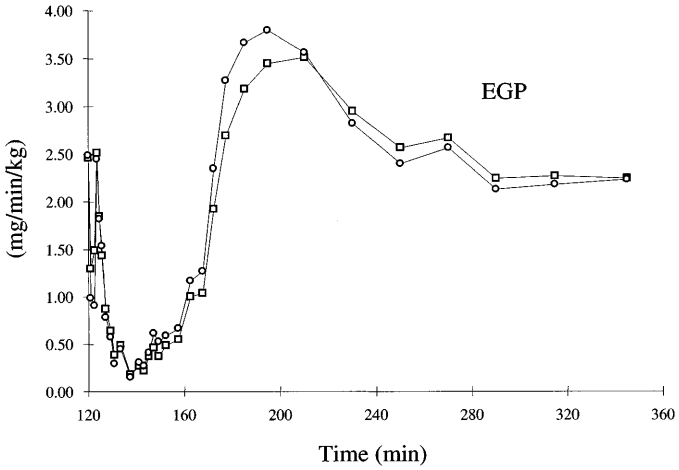

Fig. 4. TTR clamp estimates of endogenous glucose production (EGP) obtained with 2-compartment model of Radziuk et al. (20) (○) and with single-compartment model of Steele et al. (22) (□).

difficult, because the time of resumption of EGP varied among the subjects. Moreover, when both tracer and endogenous glucose concentrations are very low, such as during maximal inhibition, the time course of the TTR is very sensitive to changes in both tracer and glucose concentration. Therefore, if a small increase in endogenous glucose concentration is not accompanied by a concomitant increase in the tracer concentration (as dictated off-line by the exogenous infusion), this would induce a noticeable decrease in the TTR. Now, the problem is to determine in some way to what extent these problems related to the TTR clamp introduced an error in our estimate of EGP between 200 and 360 min. As a possible approach to at least partially assess the magnitude of this error, we compared EGP calculated with the model of Steele (22) (setting the volume of the glucose compartment equal to 1.3 dl/kg body wt and individualizing the basal value of the irreversible, time-varying loss from this volume and plasma clearance rate) with that of the model of Radziuk et al. (20). In fact, because theory shows (6) that the error affecting EGP estimation depends on both the model used for non-steady-state glucose kinetics and the rate of change of the TTR, the difference between the models of Radziuk et al. and Steele (i.e., between a good and a poor model of non-steady-state glucose kinetics) provides some insight on the influence of the TTR changes on the estimate of EGP. The time courses of EGP thus derived were almost superimposable (Fig. 4); therefore, despite an imperfect clamp of specific activity, it is possible to conclude that the EGP estimate calculated between 200 and 360 min is reliable.

The sudden up-and-down performance of EGP observed with both models in the first 10 min of the IVGTT is unlikely to be representative of a true physiological occurrence. Rather, it is probably a symptom of the marked ill-conditioning affecting EGP estimation in that portion of the IVGTT. We speculate that, even in the presence of a good TTR clamp and data smoothing, when sampling is very frequent and the tracer infusion rate is frequently changed, as in the initial part of the IVGTT, even very small errors in the evaluation of the TTR derivative are uncontrollably amplified and determine spurious oscillations in the deconvolved profile.

Deconvolution

The uniquely identifiable parameters of the 2CMM were estimated from [6,6-$^2H_2$]glucose data by weighted nonlinear least squares as described in Ref. 24. The model was identified in all subjects (Table 2). The measurement error coefficient of variation (CV) of [6,6-$^2H_2$]glucose concentration data ranged from 2.3 to 12.6% on average, with lower precision associated with lower concentration values. The mean EGP time course estimated by deconvolution is shown in Fig. 5 together with that obtained with the TTR clamp (mean ± SE). We can see that, on average, there is a very good accordance between the two estimates. EGP is almost completely inhibited already at 140 min, and early in the test it clearly shows a bimodal pattern, probably caused by the insulin injection between 140 and 145 min [a plot of the average insulin action x(t) estimated by the model is shown in Fig. 6]. The exogenous insulin administration results then in a new suppression of EGP,

Table 2. *Two-compartment minimal model parameters identified from IVGTT data of [6,6-$^2H_2$]glucose data with assumption of insulin and glucose plasma concentrations as known inputs*

Subject No.	V_1, dl/kg	k_{21}, min^{-1}	k_{12}, min^{-1}	k_{02}, min^{-1}	p_2, min^{-1}	s_k, $ml \cdot min^{-1} \cdot \mu U^{-1}$
1	2.47 (20)	0.042 (16)	0.338 (24)	0.0233 (207)	0.0672 (24)	0.0185 (229)
2	1.71 (4)	0.038 (15)	0.024 (39)	0.0018 (21)	0.1886 (21)	0.0025 (82)
3	2.53 (3)	0.030 (11)	0.069 (37)	0.0055 (27)	0.3930 (57)	0.0069 (71)
4	1.73 (6)	0.115 (23)	0.154 (14)	0.0032 (12)	0.0596 (11)	0.0015 (10)
5	2.37 (4)	0.064 (21)	0.181 (18)	0.0128 (20)	0.0685 (11)	0.0100 (36)
6	1.87 (11)	0.110 (57)	0.350 (22)	0.0071 (36)	0.1323 (18)	0.0035 (58)
7	2.17 (8)	0.065 (9)	0.232 (91)	0.0089 (70)	0.0961 (10)	0.0104 (92)
8	1.99 (6)	0.043 (23)	0.060 (21)	0.0042 (18)	0.0689 (23)	0.0052 (41)
9	1.69 (8)	0.064 (28)	0.074 (21)	0.0035 (9)	0.1071 (24)	0.0025 (16)
10	1.45 (9)	0.218 (21)	0.188 (10)	0.0033 (14)	0.0512 (9)	0.0013 (8)
Mean ± SE	2.00 ± 0.12	0.079 ± 0.018	0.167 ± 0.036	0.0074 ± 0.0021	0.1232 ± 0.0327	0.0062 ± 0.0017

Values are parameter estimates. Numbers in parentheses are estimate precisions expressed as %CV. IVGTT, intravenous glucose tolerance test; p_2 and s_k, insulin action parameters.

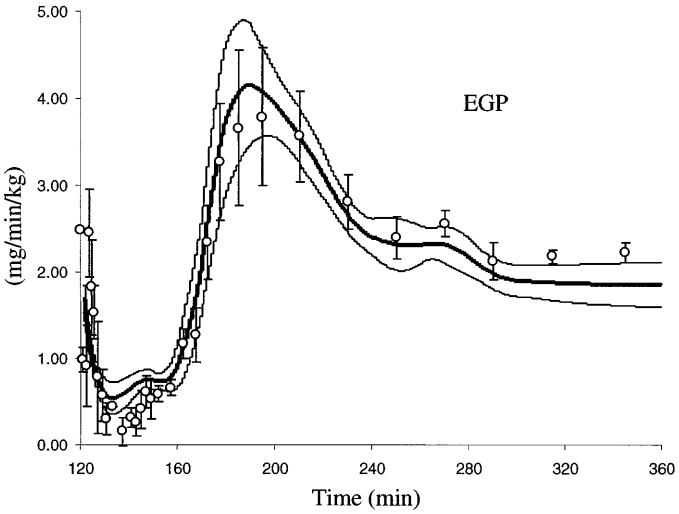

Fig. 5. EGP estimated by deconvolution (thick line) and by TTR clamp and 2-compartment model of Radziuk et al. (20) (○). Standard errors are shown by thin lines and error bars.

even if EGP is already almost completely inhibited by the glucose bolus alone. Resumption to baseline is accompanied by a consistent overshoot of EGP, well above basal, which is probably driven by the counterregulatory hormones. A comparison of the timing of EGP dynamics evaluated with the two approaches and of the extent of EGP overshoot is given in Table 3. It should be noted that resumption to baseline is rather variable (both in timing and extent) among individuals, so that endogenous glucose TTR could not always be kept precisely constant at the time of resumption (see also Fig. 3). An experimental design adjustable from subject to subject would in principle have been valuable, but mass spectrometry measurements are not feasible on-line.

It is of interest to note that the 2CMM accurately assesses the dynamics of EGP during the IVGTT but provides an estimate of basal EGP that is lower than that independently calculated from [U-^{13}C]glucose data in the steady state before the IVGTT (EGP_b = 2.47 ± 0.15 vs. 1.89 ± 0.19 mg·kg^{-1}·min^{-1}, $P < 0.05$ from paired, two-tailed *t*-test). Because basal EGP is the product of basal glucose clearance times basal glucose concentration, the underestimation of EGP might reflect an underestimation of basal glucose clearance by the 2CMM analysis. Given that the estimation of basal glucose clearance by the 2CMM hinges on the final part of the tracer disappearance curve (when insulin action is almost negligible and glucose is close to its basal level), a preliminary question must be addressed before concluding that the 2CMM provides a biased estimate of glucose clearance: is it true that glucose clearance in the final part of the test is similar to that in the pretest? An answer to this question comes from the analysis of [U-^{13}C]glucose data: the mean value of glucose clearance that is assessed from the model of Radziuk et al. (20) in the final part of the IVGTT [calculated as the product $k_{01}(t)\cdot V_1$] is not different from that measured with the same tracer before the IVGTT (2.90 ± 0.56 vs. 2.47 ± 0.46, not significant). This result allows us to conclude that for some reason the 2CMM identified from [6,6-$^2H_2$]glucose data underestimates the glucose clearance achieved at the end of the IVGTT. The next step is to localize the source of error: is there a problem in the model or in the [6,6-$^2H_2$]glucose data? We have come to the conclusion that the problem is in the [6,6-$^2H_2$]glucose concentration data. This was proven by taking the last five to six data points of the [6,6-$^2H_2$]glucose disappearance curve and fitting these data with a single exponential. We reasoned that, because insulin action is low in that part of the test and glucose is close to its basal level, fitting a single exponential through the latter part of the test is a feasible method to estimate the slowest eigenvalue (λ_2) of glucose kinetics, the one that is mainly responsible for the clearance. We then compared this data-driven assessment of λ_2 to the slow eigenvalue of the 2CMM. We reasoned that if the 2CMM underestimates glucose clearance because of some model error, the model-based λ_2 should be lower than the data-driven λ_2. We found that the two values of λ_2 were virtually identical: λ_2 from the single-exponential fitting was 7.9 ± 1.6 × 10^{-2}/min and from the 2CMM was 7.2 ± 0.8 × 10^{-2}/min, r^2 = 0.78. This result indicates both that the 2CMM provides an estimate of glucose clearance that simply reflects the final IVGTT [6,6-$^2H_2$]glucose data and that [6,6-$^2H_2$]glucose data provide an estimate of glucose clearance lower than that provided by [U-^{13}C]glucose data.

A hypothesis that could account for this observation is that there is a spurious fraction of [6,6-$^2H_2$]glucose that is recirculating back from the liver, possibly due to the large resumption of EGP in the second part of the IVGTT. Glucose-carbon recycling is not a viable option, because similar values of plasma clearance rate (PCR) and EGP were estimated with protocols in absence of carbon tracers.

To gain further understanding of the 2CMM validity, we attempted to validate its description of the glucose system by the following procedure. We applied the known [U-^{13}C]glucose infusion as a known input to the

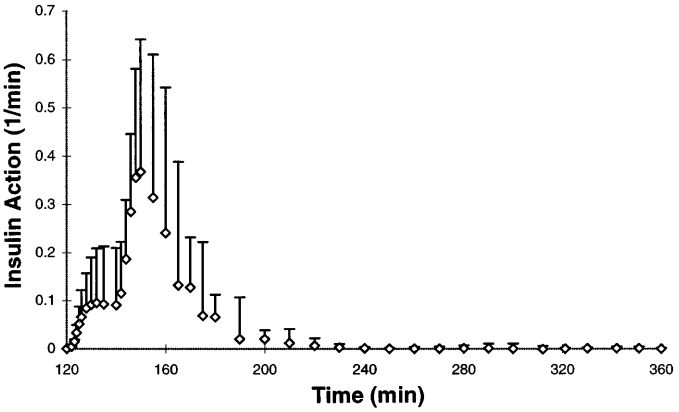

Fig. 6. Mean insulin action (min^{-1}) in remote insulin compartment estimated by 2-compartment minimal model. Error bars are standard deviations.

Table 3. *Individual comparison of salient features of EGP estimates by Radziuk and by the 2CMM*

Subject No.	EGP Estimate									
	Radziuk					2CMM				
	T_{N1}	T_{N2}	T_{cross}	ΔT_{max}	EGP_{max}	T_{N1}	T_{N2}	T_{cross}	ΔT_{max}	EGP_{max}
1	126	134	185	77	3.84	126	157	166	23	5.27
2	127	138	185	73	3.91	137	149	178	63	4.63
3	131	141	185	69	2.80	131	157	182	55	2.85
4	131	168	195	63	2.47	129	167	178	32	2.93
5	131	149	168	36	6.34	133	158	168	27	8.47
6	129	153	178	58	2.46	136	164	178	35	2.65
7	131	147	158	38	8.75	125	149	156	31	7.77
8	126	143	178	52	4.96	138	156	168	25	5.32
9	134	158	185	53	2.39	139	181	188	31	3.48
10	129	147	173	48	5.33	139	151	170	38	5.30
Mean ± SE	129 ± 1	148 ± 3	179 ± 3	56 ± 4	4.33 ± 0.65	133 ± 2	159 ± 3	173 ± 3	36 ± 4	4.87 ± 0.64

2CMM, 2-compartment minimal model; T_{N1} (min), time of first nadir; T_{N2} (min), time of second nadir or saddle point; T_{cross} (min), time at which endogenous glucose production (EGP) crosses its basal value EGP_b; ΔT_{max} (min), time elapsed between T_{N2} and time of maximum EGP overshoot; EGP_{max} ($mg \cdot min^{-1} \cdot kg^{-1}$), maximum EGP overshoot. Note that IVGTT bolus is administered at t = 120 min. For Radziuk's estimate, T_{N1}, T_{N2}, and T_{max} are defined only on midpoints of sampling grid, whereas for 2CMM estimate they can lie anywhere within sampling interval.

2CMM identified from [6,6-$^2H_2$]glucose data, and then we compared the model output with the measured [U-^{13}C]glucose concentration data. We reasoned that, if the model identified from the [6,6-$^2H_2$]glucose dynamics was able to account for the observed [U-^{13}C]glucose data, this would support its validity. It can be seen from the results reported in Fig. 7 that the match between data and model is quite good except for the final part of the IVGTT, where the model prediction tends to overestimate the observed data. This results in additional evidence that the 2CMM underestimates glucose clearance in the final part of the IVGTT.

Our results also provide some new insight into the control of glucose and insulin on EGP suppression. In the first 40 min after the start of the IVGTT, EGP shows a bimodal pattern, that is, it is almost totally inhibited already 15–20 min after the glucose challenge, then slightly but quickly resumes, and is again inhibited at ~30–35 min (see Table 3). This second nadir is in all likelihood due to the exogenous insulin infusion. It is interesting to note, however, that EGP is already almost completely suppressed before the insulin injection; thus, it is likely that the insulin injection pushes further a process that is already fully inhibited. There is also a very high interindividual variability in both the timing and the entity of EGP resumption to baseline, as demonstrated by Table 3 and the error bars in Fig. 5, and this is confirmed by both methods.

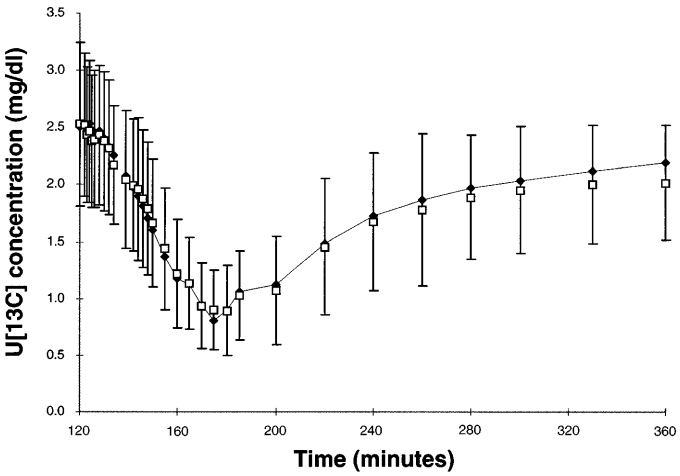

Fig. 7. Results of applying the known [U-^{13}C]glucose infusion as a known input to the 2-compartment minimal model (2CMM) identified from [6,6-$^2H_2$]glucose data. Model prediction (◆) is shown together with experimental [U-^{13}C]glucose concentration data (□ with SD error bars).

Finally, the time course of EGP allows us to qualitatively answer the question of whether EGP inhibition is triggered directly by plasma glucose concentration. Apart from the values at 122 and 123 min, which apparently show a fast EGP inhibition and a quick return to basal but are in all likelihood spurious (see earlier discussion), EGP is suppressed slowly with respect to the time course of plasma glucose concentration, and this rules out the possibility that EGP inhibition is directly proportional to plasma glucose. It therefore seems more likely that some delayed glucose signal is responsible for EGP inhibition.

Conclusions

We have validated the estimate of EGP during an IVGTT obtained by deconvolution against a model-independent estimate obtained with the TTR clamp. Both approaches demonstrated almost complete suppression of EGP within 20 min and a high interindividual variability in the resumption to baseline. The time course of EGP calculated with both approaches compared very well. Thus the 2CMM, in addition to providing metabolic indexes of glucose effectiveness and insulin sensitivity, also recovers, when used in conjunction with deconvolution, EGP time course during the IVGTT; it therefore is a potentially very useful tool to assess glucose metabolism in vivo.

APPENDIX

Appendix A: EGP Estimate from TTR Clamp

Equations of the model of Radziuk et al. (20) for endogenous glucose (tracee) kinetics during the IVGTT are

$$\frac{dq_1(t)}{dt} = -[k_{01}(t) + k_{21}]q_1(t) + k_{12}q_2(t) + EGP(t) \qquad q_1(0) = G_bV_1$$

$$\frac{dq_2(t)}{dt} = k_{21}q_1(t) - k_{12}q_2(t) \qquad q_2(0) = G_bV_1\frac{k_{21}}{k_{12}} \tag{A1}$$

$$G_e(t) = \frac{q_1(t)}{V_1}$$

where q_1 and q_2 denote endogenous glucose masses (mg/kg) in the first and second compartments, respectively, V_1 is the volume of the accessible pool (dl/kg), G_b is basal (pretest) glucose concentration, and k_{21} (min^{-1}), k_{12} (min^{-1}), and k_{01} (min^{-1}) are rate parameters describing glucose kinetics.

Equations for the tracer [U-^{13}C]glucose (C_{II}) kinetics are

$$\frac{dq_1^*(t)}{dt} = -[k_{01}(t) + k_{21}]q_1^*(t) + k_{12}q_2^*(t) + R_a^*(t) \qquad q_1^*(0) = C_{II}(0)V_1$$

$$\frac{dq_2^*(t)}{dt} = k_{21}q_1^*(t) - k_{12}q_2^*(t) \qquad q_2^*(0) = C_{II}(0)V_1\frac{k_{21}}{k_{12}} \tag{A2}$$

$$C_{II}(t) = \frac{q_1^*(t)}{V_1}$$

where the superscript * denotes tracer-related variables, and $C_{II}(0)$ is different from zero, because by experimental design [U-^{13}C]glucose has already reached a constant level in plasma before the initiation of the IVGTT.

A priori identifiable model parameters are V_1, k_{21}, k_{12}, and the basal value of $k_{01}(t)$, k_{01}. Glucose plasma clearance rate PCR and basal EGP, EGP_b, can be directly calculated from the model parameters as

$$PCR = k_{01}V_1 \tag{A3}$$

and

$$EGP_b = PCR\ G_b \tag{A4}$$

respectively.

Let us calculate now EGP from the model of Radziuk et al. (20). Rearranging the tracee equations, we can derive an expression for EGP(t)

$$EGP(t) = \frac{dq_1(t)}{dt} + [k_{01}(t) + k_{21}]q_1(t) - k_{12}q_2(t) \tag{A5}$$

and from the definition of TTR

$$q_1(t) = \frac{q_1^*(t)}{Z_{II}(t)} \tag{A6}$$

Substituting in *Eq. A5* the expression for k_{01} obtained from *Eqs. A1* and *A2*, we obtain

$$EGP(t) = \frac{dq_1(t)}{dt} + \frac{1}{Z_{II}(t)}\left[R_a^*(t) - \frac{dq_1^*(t)}{dt} + k_{12}q_2^*(t)\right] - k_{12}q_2(t) \tag{A7}$$

from which, rearranging, we obtain the final expression for EGP

$$EGP(t) = \frac{R_a^*(t)}{Z_{II}(t)} - \frac{V_1G_e(t)}{Z_{II}(t)}\frac{dZ_{II}(t)}{dt} + k_{12}\left[\frac{q_2^*(t)}{Z_{II}(t)} - q_2(t)\right] \tag{A8}$$

Now, $q_2^*(t)$ is the mass of tracer glucose in the accessible pool, and $q_2(t)$ is the mass of tracee glucose in the second, nonaccessible pool. Whereas $q_1(t)$ (q_1^*) was calculated at each sampling point by multiplying the endogenous (exogenous) glucose concentration by V_1, i.e., the volume of the accessible pool, $q_2(t)$ (q_2^*) was calculated at each sampling point by solving the first-order differential equation with constant parameters that describe the kinetics of the Radziuk model's second pool. This differential equation has $q_1(t)$ (q_1^*) as forcing input. The time course (continuous) of $q_1(t)$ (q_1^*) was calculated by linear interpolation.

Appendix B: EGP Estimate by Deconvolution

The 2CMM is described by Refs. 5, 10, and 24

$$\frac{dq_1^*(t)}{dt} = -\left[k_p + \frac{R_{d,0}}{q_1(t)} + k_{21}\right]q_1^*(t) + k_{12}q_2^*(t) \qquad q_1^*(0) = D^*$$

$$\frac{dq_2^*(t)}{dt} = k_{21}q_1^*(t) - [k_{02} + x(t) + k_{12}]q_2^*(t) \qquad q_2^*(0) = 0 \tag{B1}$$

$$\frac{dx(t)}{dt} = -p_2x(t) + s_k[I(t) - I_b] \qquad x(0) = 0$$

$$C_I(t) = \frac{q_1^*(t)}{V_1}$$

where q_1^* and q_2^* denote [6,6-$^2H_2$]glucose masses in the first (accessible pool) and second (slowly-equilibrating) compartments, respectively (mg/kg), x(t) is insulin action (min^{-1}), I(t) and I_b are plasma insulin and basal (endtest) insulin, respectively (μU/ml), G_b is basal (endtest) glucose concentration (mg/dl), $q_1(t)$ is cold glucose mass in the accessible pool (mg/dl), $C_I(t)$ is plasma [6,6-$^2H_2$]glucose concentration (mg/dl), D^* is the hot glucose dose (mg/kg), V_1 is the volume of the accessible pool (dl/kg), and k_{21} (min^{-1}), k_{12} (min^{-1}), k_{02} (min^{-1}), p_2 (min^{-1}), and s_k ($\mu U \cdot ml^{-1} \cdot min^{-1}$) are rate parameters describing glucose kinetics and insulin action.

Briefly, the model structure assumes that insulin-independent glucose disposal takes place in the accessible pool and is the sum of two components, one constant (due to, e.g., central nervous system and red blood cells) and the other proportional to glucose mass. This brings us to the rate constant describing the irreversible loss from the accessible pool

$$k_{01}(t) = k_p + \frac{R_{d,0}}{G(t)V_1} \qquad (B2)$$

where G(t) is the glucose concentration in the accessible pool of volume V_1, $R_{d,0}$ ($mg \cdot kg^{-1} \cdot min^{-1}$) is the constant component of glucose disposal, and k_p (min^{-1}) accounts for the proportional-to-mass term.

To arrive at a priori uniquely identifiable parameters, it is assumed that *1*) in the basal steady state, insulin-independent glucose disposal (from *compartment 1*) is three times insulin-dependent glucose disposal (from *compartment 2*), and *2*) $R_{d,0}$ is fixed to the experimentally determined value (2) of 1 $mg \cdot kg^{-1} \cdot min^{-1}$; this brings us to the following relation among the model parameters

$$k_p + \frac{R_{d,0}}{G_b V_1} = \frac{3k_{21}k_{02}}{k_{02} + k_{12}} \qquad (B3)$$

The uniquely identifiable parameters of the 2CMM are six: V_1, k_{21}, k_{12}, k_{02}, p_2, and s_k. From the model parameters, it is possible to calculate basal EGP

$$EGP_b = R_{d,0} + V_1\left(k_p + \frac{k_{21}k_{02}}{k_{02} + k_{12}}\right)G_b \qquad (B4)$$

The estimate of EGP during the IVGTT nonsteady state was obtained by describing with the 2CMM the impulse response h(t,τ) of the glucose system, and by applying a deconvolution algorithm to invert the integral relation of *Eq. 6*. The deconvolution approach used here is nonparametric, is described in Refs. 12 and 24, and was previously used to reconstruct insulin secretion during an IVGTT (21). We refer to these works for details. An advantage of the method consists in the availability of a new statistically sound criterion, based on maximum likelihood, for the choice of the regularization parameter.

The authors thank Dr. Gianna M. Toffolo, of the Department of Electronics and Informatics of the University of Padova, for helpful collaboration in the interpretation of the mass spectrometry measurements.

This work was partially supported by a grant from the Italian Ministero della Università e della Ricerca Scientifica e Tecnologica (MURST 40%) on "Biosistemi e Bioinformatica," by Grant 9300457PF40 from the Italian National Research Council (CNR) on "Aging," and by National Institutes of Health Grants RR-02176, RR-11095, RR-00954, RR-00036, and DK-49393.

Present address of P. Vicini: Department of Bioengineering, University of Washington, Seattle, WA 98195.

Address for reprint requests: C. Cobelli, Dept. of Electronics and Informatics, Univ. of Padova, Via Gradenigo 6/A, 35131 Padova, Italy.

Received 16 December 1997; accepted in final form 9 October 1998.

REFERENCES

1. **Avogaro, A., P. Vicini, A. Valerio, A. Caumo, and C. Cobelli.** The hot but not the cold minimal model allows precise assessment of insulin sensitivity in NIDDM subjects. *Am. J. Physiol.* 270 (*Endocrinol. Metab.* 33): E532–E540, 1996.
2. **Best, J. D., J. Taborsky, Jr., J. B. Halter, and D. Porte, Jr.** Glucose disposal is not proportional to plasma glucose level in man. *Diabetes* 30: 847–850, 1981.
3. **Carson, E. R., C. Cobelli, and L. Finkelstein.** *The Mathematical Modeling of Metabolic and Endocrine Systems.* New York: Wiley, 1983.
4. **Caumo, A., and C. Cobelli.** Hepatic glucose production during the labeled IVGTT: estimation by deconvolution with a new minimal model. *Am. J. Physiol.* 264 (*Endocrinol. Metab.* 27): E829–E841, 1993.
5. **Caumo, A., A. Giacca, M. Morgese, G. Pozza, P. Micossi, and C. Cobelli.** Minimal model of glucose disappearance: lessons from the labeled IVGTT. *Diab. Med.* 8: 822–832, 1991.
6. **Cobelli, C., A. Mari, and E. Ferrannini.** Non-steady state: error analysis of Steele's model and developments for glucose kinetics. *Am. J. Physiol.* 252 (*Endocrinol. Metab.* 15): E679–E689, 1987.
7. **Cobelli, C., and G. Toffolo.** Constant specific activity input allows reconstruction of endogenous glucose concentration in non-steady state. *Am. J. Physiol.* 258 (*Endocrinol. Metab.* 21): E1037–E1040, 1990.
8. **Cobelli, C., G. Toffolo, D. M. Bier, and R. Nosadini.** Models to interpret kinetic data in stable isotope tracer studies. *Am. J. Physiol.* 253 (*Endocrinol. Metab.* 16): E551–E564, 1987.
9. **Cobelli, C., G. Toffolo, and D. M. Foster.** Tracer-to-tracee ratio for analysis of stable isotope tracer data: link with radioactive kinetic formalism. *Am. J. Physiol.* 262 (*Endocrinol. Metab.* 25): E968–E975, 1992.
10. **Cobelli, C., P. Vicini, G. Toffolo, and A. Caumo.** The hot IVGTT minimal models: simultaneous assessment of disposal indices and endogenous glucose production. In: *The Minimal Model Method and Determinants of Glucose Tolerance,* edited by J. Lovejoy and R. N. Bergman. Baton Rouge, LA: Louisiana State University Press, p. 202–239, 1998. (Pennington Nutr. Ser.)
11. **Cowan, J. R., and G. Hetenyi, Jr.** Glucoregulatory responses in normal and diabetic dogs recorded by a new tracer method. *Metab. Clin. Exp.* 20: 360–372, 1971.
12. **De Nicolao, G., G. Sparacino, and C. Cobelli.** Nonparameteric input estimation in physiological systems: problems, methods, case studies. *Automatica* 33: 851–870, 1997.
13. **Fick, A.** Über die Messung des Blutquantums in den Herzventrikeln. *Verhandl Phys. Med. Ges. Wurzburg* 2: XVI, 1870.
14. **Finegood, D. T., R. N. Bergman, and M. Vranic.** Estimation of endogenous glucose production during hyperinsulinemic-euglycemic glucose clamps: comparison of unlabeled and labeled exogenous glucose infusates. *Diabetes* 36: 914–924, 1987.
15. **Finegood, D. T., I. M. Hramiak, and J. Duprè.** A modified protocol for estimation of insulin sensitivity with the minimal model of glucose kinetics in patients with insulin dependent diabetes. *J. Clin. Endocrinol. Metab.* 70: 1538–1548, 1990.
16. **Hales, C., and P. J. Randle.** Immunoassay of insulin with insulin antibody precipitate. *Biochem. J.* 88: 137–146, 1963.
17. **Jacquez, J. A.** Theory of production rate calculations in steady and non-steady states and its application to glucose metabolism. *Am. J. Physiol.* 262 (*Endocrinol. Metab.* 25): E779–E790, 1992.
18. **Norwich, K. N.** Measuring rates of appearance in systems which are not in steady state. *Can. J. Physiol. Pharmacol.* 51: 91–101, 1973.
19. **Overkamp, D., J. F. Gautier, W. Renn, A. Pickert, A. J. Scheen, R. M. Schmulling, M. Eggstein,† and P. J. Lefebvre.** Glucose turnover in humans in the basal state and after intravenous glucose: a comparison of two models. *Am. J. Physiol.* 273 (*Endocrinol. Metab.* 36): E284–E296, 1997.
20. **Radziuk, J., K. H. Norwich, and M. Vranic.** Experimental validation of measurements of glucose turnover in nonsteady

state. *Am. J. Physiol.* 234 (*Endocrinol. Metab. Gastrointest. Physiol.* 3): E84–E93, 1978.
21. **Sparacino, G., and C. Cobelli.** A stochastic deconvolution method to reconstruct insulin secretion rate after a glucose stimulus. *IEEE Trans. Biomed. Eng.* 435: 512–529, 1996.
22. **Steele, R.** Influence of glucose loading and of injected insulin on hepatic glucose output. *Ann. NY Acad. Sci.* 82: 420–430, 1959.
23. **Vicini, P., A. Caumo, and C. Cobelli.** The hot IVGTT two compartment minimal model: indexes of glucose effectiveness and insulin sensitivity. *Am. J. Physiol.* 273 (*Endocrinol. Metab.* 36): E1024–E1032, 1997.
24. **Vicini, P., G. Sparacino, A. Caumo, and C. Cobelli.** Estimation of EGP after a glucose perturbation by nonparametric stochastic deconvolution. *Comput. Methods Prog. Biomed.* 52: 147–156, 1997.
25. **Yang, Y. J., J. H. Youn, and R. N. Bergman.** Modified protocols improve insulin sensitivity estimation using the minimal model. *Am. J. Physiol.* 253 (*Endocrinol. Metab.* 16): E595–E602, 1987.
26. **Zierler, K. L.** Theory of the use of arteriovenous concentration differences for measuring metabolism in steady and nonsteady states. *J. Clin. Invest.* 40: 2111–2125, 1961.